AD-A137 132 NONLINEAR THEORY OF THE E X INSTABILITY WITH AN INHOMOGENEOUS ELECTRIC FIELD(U) NAVAL RESEARCH LAB WASHINGTON DC M J KESKINEN 09 JAN 84 NRL-MR-5235 1/1

UNCLASSIFIED F/G 12/1 NL

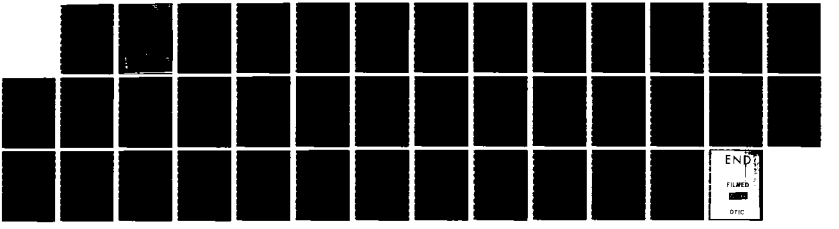

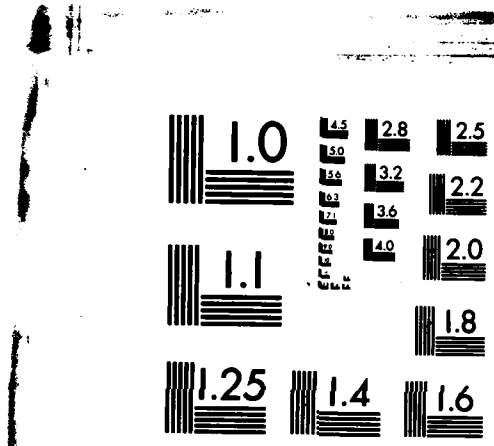

NRL Memorandum Report 5235

Nonlinear Theory of the E × B Instability with an Inhomogeneous Electric Field

M. J. KESKINEN

Geophysical and Plasma Dynamics Branch
Plasma Physics Division

January 9, 1984

This research was sponsored by the Defense Nuclear Agency under Subtask S99QMXBC, work unit 00067, work unit title "Plasma Structure Evolution" and by the Office of Naval Research.

NAVAL RESEARCH LABORATORY
Washington, D.C.

SECURITY CLASSIFICATION OF THIS PAGE (When Data Entered)

REPORT DOCUMENTATION PAGE	READ INSTRUCTIONS BEFORE COMPLETING FORM
1. REPORT NUMBER: NRL Memorandum Report 5235	2. GOVT ACCESSION NO. / 3. RECIPIENT'S CATALOG NUMBER
4. TITLE (and Subtitle): NONLINEAR THEORY OF THE E × B INSTABILITY WITH AN INHOMOGENEOUS ELECTRIC FIELD	5. TYPE OF REPORT & PERIOD COVERED: Interim report on a continuing NRL problem.
	6. PERFORMING ORG. REPORT NUMBER
7. AUTHOR(s): M.J. Keskinen	8. CONTRACT OR GRANT NUMBER(s)
9. PERFORMING ORGANIZATION NAME AND ADDRESS: Naval Research Laboratory, Washington, DC 20375	10. PROGRAM ELEMENT, PROJECT, TASK AREA & WORK UNIT NUMBERS: 62715H; 61153N; 47-0889-0-3; 47-0883-0-3
11. CONTROLLING OFFICE NAME AND ADDRESS: Defense Nuclear Agency, Washington, DC 20305; Office of Naval Research, Arlington, VA 22203	12. REPORT DATE: January 9, 1984
	13. NUMBER OF PAGES: 37
14. MONITORING AGENCY NAME & ADDRESS(if different from Controlling Office)	15. SECURITY CLASS. (of this report): UNCLASSIFIED
	15a. DECLASSIFICATION/DOWNGRADING SCHEDULE

16. DISTRIBUTION STATEMENT (of this Report)

Approved for public release; distribution unlimited.

17. DISTRIBUTION STATEMENT (of the abstract entered in Block 20, if different from Report)

18. SUPPLEMENTARY NOTES

This research was sponsored by the Defense Nuclear Agency under Subtask S99QMXBC, work unit 00067, work unit title "Plasma Structure Evolution" and by the Office of Naval Research.

19. KEY WORDS (Continue on reverse side if necessary and identify by block number)

E × B instability
Nonlinear theory
Inhomogeneous electric field
High latitude ionosphere

20. ABSTRACT (Continue on reverse side if necessary and identify by block number)

Using analytical and numerical techniques, the nonlinear evolution of the E × B instability with an inhomogeneous electric field has been studied. For the case where the electric field component parallel to the density gradient is inhomogeneous, we find that the inhomogeneous E × B instability in the nonlinear regime (1) destabilizes short wavelength linear stable modes, (2) evolves into large scale anisotropic finger-like structures, (3) can be described by power laws, $P(k_x) \propto k_x^{-n_x}$, n_x (Continues)

DD FORM 1 JAN 73 1473 EDITION OF 1 NOV 65 IS OBSOLETE
S/N 0102-014-6601

SECURITY CLASSIFICATION OF THIS PAGE (When Data Entered)

asymptotically equal

20. ABSTRACT (Continued)

≥ 2, $P(k_\perp) \propto k_\perp^{-n_\perp}$, $n_\perp \gtrsim 2$-3 where $P(k_\perp)$ and $P(k_\parallel)$ are the one-dimensional power spectra parallel and perpendicular to the initial density gradient and (4) can be stabilized by quasilinear mechanisms in which the initial density gradient is modified by a finite amplitude wave spectrum. Applications are made both to naturally occurring small scale structures in the auroral ionosphere and striation formation in artificially produced ionospheric plasma clouds.

CONTENTS

NONLINEAR THEORY OF THE E × B INSTABILITY WITH AN INHOMOGENEOUS ELECTRIC FIELD

1. INTRODUCTION

The E x B instability, also known as the gradient-drift instability, has been invoked to explain both natural and artificially induced plasma density structure and irregularities in the terrestrial ionosphere. This instability can be excited in a low pressure, weakly ionized, magnetized plasma that contains an ambient electric field orthogonal to both a magnetic field and a density gradient. The basic physical mechanism for the E x B instability [Linson and Workman, 1970; Perkins et al., 1973] is analogous to that describing the classical Rayleigh-Taylor instability in which a heavy fluid is supported by a lighter fluid. Originally applied by Simon [1963] and Hoh [1963] to laboratory gas discharges, this instability has been applied to ionospheric plasma cloud structuring [Haerendel et al., 1967; Linson and Workman, 1970; Völk and Haerendel, 1971; Perkins et al., 1973; Zabusky et al., 1973; Scannapieco et al., 1976; Ossakow et al., 1978; Chaturvedi and Ossakow, 1979; Keskinen et al., 1980; McDonald et al., 1981] and to the stability and transport of large scale convecting auroral ionospheric plasma enhancements [Keskinen and Ossakow, 1982, 1983; Vickrey et al., 1980]. However, these studies have addressed only the E x B instability driven by initial ambient homogeneous electric field. Perkins and Doles [1975] have shown, using linear theory, that sheared velocity flow (resulting from an initially self-consistent inhomogeneous electric field parallel to the density gradient) can stabilize the E x B instability in the collisional regime. Huba et al. [1983] verified numerically the results of Perkins and Doles [1975] and extended the linear theory of the E

Manuscript approved October 3, 1983.

x $\underline{B}$ instability with an inhomogeneous electric field to the collisionless regime. In order to properly apply the $\underline{E}$ x $\underline{B}$ instability to the auroral and polar ionosphere and magnetosphere one must consider the linear and nonlinear evolution of the $\underline{E}$ x $\underline{B}$ instability with an inhomogeneous electric field since it is well known that high latitude magnetospheric and ionospheric electric fields are usually inhomogeneous [see, for example, Fairfield, 1977 and references therein].

The purpose of this paper is to study the nonlinear evolution of the $\underline{E}$ x $\underline{B}$ instability with an inhomogeneous electric field. The organization of the paper is as follows. In Section 2 we give the general equations describing the $\underline{E}$ x $\underline{B}$ instability with an inhomogeneous electric field. In Section 3 we study the nonlinear evolution of the $\underline{E}$ x $\underline{B}$ instability with inhomogeneous electric field by numerically solving the fundamental fluid equations. In Section 4 we give a nonlinear analytic theory of the results in Section 3. Finally, in Section 5 we discuss and summarize our findings.

2. MODEL EQUATIONS AND LINEAR THEORY

The basic equations describing the evolution of the $\underline{E}$ x $\underline{B}$ instability in an inhomogeneous electric field are:

$$\frac{\partial N_\alpha}{\partial t} + \nabla\cdot\left(N \underline{V}_\alpha\right) = 0 \tag{1}$$

$$-\frac{e}{m_e}\left(\underline{E} + c^{-1}\underline{V}_e \times \underline{B}\right) = 0 \tag{2}$$

$$\frac{e}{m_i}\left(\underline{E} + c^{-1}\underline{V}_i \times \underline{B}\right) - \nu_{in}\,\underline{V}_i = 0 \tag{3}$$

$$\nabla\cdot\underline{J} = \nabla\cdot N\left(\underline{V}_i - \underline{V}_e\right) = 0 \tag{4}$$

where α denotes species (α = e,i) and other symbols retain their conventional meaning.

The equilibrium configuration used in the analysis is shown in Fig. 1. The ambient magnetic and electric fields are in the z direction and the x,y plane, respectively, where $\underset{\sim}{B} = B_o \hat{\underline{z}}$ and $\underset{\sim}{E} = E_{ox}(x)\ \hat{\underline{x}} + E_{oy}\ \hat{\underline{y}}$. The electric field in the y direction is constant, while the electric field in the x direction is allowed to be a function of x. This gives rise to an inhomogeneous velocity flow in the y direction, i.e., $V_{oy}(x) = -cE_{ox}(x)/B$. The density is taken to be inhomogeneous in the x direction ($n_o = n_o(x)$) and temperature effects are ignored.

The basic assumptions used in the analysis are as follows. We assume that the perturbed quantities vary as $\delta f \sim \delta f(x) \exp[i(k_y y - \omega t)]$, where k_y is the wave number along y direction and $\omega = \omega_r + i\gamma$, implying growth for $\gamma > 0$. The ordering in the frequencies is such that $\omega << \Omega_i$ and $\nu_{in} << \Omega_i$ (F region approximation), where ν_{in} is the ion-neutral collision fre-quency and Ω_i is the ion gyrofrequency. We ignore finite gyroradius effects by limiting the wavelength domain to $kr_{Li} << 1$, where r_{Li} is the mean ion Larmor radius. We neglect perturbations along the magnetic field $(k_\parallel = 0)$ so that only the two-dimensional structure in the x,y plane is obtained.

Solving Eq. (2) and (3) for $\underline{V_e}$ and $\underline{V_i}$, substituting into (1) (for electrons) and (4) we find [Perkins and Doles, 1975]

$$\frac{\partial N}{\partial t} + \underline{V}_{oy} \cdot \nabla N - \frac{c}{B}\ \nabla\delta\phi \times \hat{\underline{z}} \cdot \nabla N = 0 \tag{5}$$

$$\nabla \cdot N \nabla \delta\phi = - E_{oy} \frac{\partial N}{\partial y} - \frac{\partial}{\partial x}\left(E_{ox}(x) N\right) \tag{6}$$

where we have transformed to a frame moving with velocity $\underline{V}_o = -\frac{c}{B} E_{oy} \hat{x}$, let $N = n_o(x) + \delta n$, $\underline{E} = E_{ox}(x)\hat{x} + E_{oy}\hat{y} - \nabla\delta\phi$, and $\underline{V}_{oy}(x) = -cE_{ox}(x)/B\,\hat{y}$. A relationship between initial equilibrium $n_o(x)$ and $E_{ox}(x)$ can be found by assuming $\nabla\cdot\underline{J} = 0$ from Eq. (4) or (6) which gives

$$n_o(x)E_{ox}(x) = \text{cst.} \tag{7}$$

where we take the constant to be the left hand side of Eq. (7) evaluated at $x = -\infty$. Adopting a Fourier representation in Eq. (5), (6) for δn, $\delta\phi$, eliminating δn from Eq. (6) using Eq. (5) we find the dispersion relation

$$\frac{\partial^2 \delta\phi_{\underline{k}}}{\partial x^2} + A(k_y, x, \omega)\frac{\partial \delta\phi_{\underline{k}}}{\partial x} + B(k_y, x, \omega)\delta\phi_{\underline{k}} = 0 \tag{8}$$

where

$$A(k_y,x,\omega) = \frac{1}{n_o}\frac{dn_o}{dx}\left[1 + k_y V_{oy}(x)(\omega - k_y V_{oy})^{-1}\right]$$

$$B(k_y,x,\omega) = -k_y^2 + i\,k_y\left(\frac{cE_{oy}}{B}\right)k_y\frac{1}{n_o}\frac{dn_o}{dx}(\omega - k_y V_{oy})^{-1}$$

$$+ k_y V_{oy}(\omega - k_y V_{oy})^{-1}\left[\frac{1}{n_o}\frac{d^2 n_o}{dx^2} - k_y\frac{1}{n_o}\frac{dn_o}{dx}\frac{dV_{oy}}{dx}(\omega - k_y V_{oy})^{-1}\right]$$

Perkins and Doles (1975) expand Eq. (8) about $x = x_o$ where x_o is the position of maximum n_o'/n_o by taking ($f' \equiv df/dx$)

$$n_o'/n_o = \left[1-(x-x_o)^2/D^2\right]/L_n \tag{9}$$

Assuming $k_y^2 L_n^2 >> 1$ and $k_y^2 D^2 << 1$, and by making several variable changes, they solve Eq. (8) analytically. The important conclusion of their results is that the $\underline{E} \times \underline{B}$ instability is stabilized, in the linear regime, when

$$\frac{E_x(x_o)}{E_y} > \frac{2}{k_y D} \tag{10}$$

Thus, the influence of velocity shear, i.e., an inhomogeneous E_{ox}, is to preferentially stabilize the short wavelength modes, i.e., those with $k_y D >> 1$. Huba et al. [1983] verified Eq. (10) by solving numerically the fully nonlocal equation (8).

To recover the local theory limit we let $\frac{\partial}{\partial x} \rightarrow ik_x$ and assume $k_x^2 L_N^2 >> 1$ and $k_y^2 L_N^2 >> 1$ where $L_N = (n_o'/n_o)^{-1}$ is the scale length of the density inhomogeneity evaluated at $x = x_o$. For simplicity we also take $\underline{E} = E_{ox}\,\hat{\underline{x}} + E_{oy}\,\hat{\underline{y}} = \text{constant}$. Following standard techniques, we find for the frequency and growth rate

$$\omega_r = k_y V_{oy} \tag{11}$$

$$\gamma = \frac{k_y}{k} \frac{\left(\underline{k} \cdot \frac{c}{B} \underline{E}\right)}{k L_N} \tag{12}$$

the usual $\underline{E} \times \underline{B}$ instability growth rate [Linson and Workman, 1970] in the collisional limit.

3. NONLINEAR EVOLUTION

Since the $\underline{E} \times \underline{B}$ instability becomes highly nonlinear and analytically intractable we will study the nonlinear evolution of the $\underline{E} \times \underline{B}$ instability in an inhomogeneous electric field by numerically solving the fundamental equations (5) and (6). We choose parameters typical of naturally occurring high latitude convecting ionospheric plasma enhancements [Vickrey et al., 1980] and artificially produced ionospheric plasma clouds [McDonald et al., 1981]. Equations (5) and (6) were solved on a numerical grid consisting of 258 grid points in the x-direction and 102 grid points in the y-direction with constand grid spacing of 0.3 km in the x-direction and 0.2 km in the y-direction. As a result, the simulation plane has an x,y extent of 80 and 20 km, respectively. The plasma density N in equation (5) was advanced in time using a multi-dimensional flux-corrected variable timestep leapfrog-trapezoid scheme [Zalesak, 1979] which is second order in time and fourth order in space. At each timestep the self-consistent electrostatic potential $\delta\phi$ of the plasma enhancement in Eq. (6) was deter-mined using a Chebychev iterative method [McDonald, 1980] with a convergence criterion of 10^{-4}. Periodic boundary conditions were imposed in the y-direction with Neumann boundary conditions ($\partial/\partial x = 0$) in the x-direction. A slab approximation is used to model the zeroth order plasma density with profile given by $n_o(x) = N_o \{1 + 4.5[\tanh(x-x_1)/L_N + \tanh(x_2-x)/L_N]\} \{1 + \varepsilon(x,y)\}$ with $x_1 = 10$ km, $x_2 = 35$ km, and $L_N = 10$ km. This gives a maximum plasma density to background ratio of approximately 10. The initial perturbation in taken to be completely random with root-mean-square amplitude of 10^{-4}.

The ambient electric field is chosen to be

$$\underset{\sim}{E}_o(x) = E_{ox}(x)\,\hat{\underline{x}} + E_{oy}\,\hat{\underline{y}} \tag{13}$$

where

$$\underset{\sim}{E}_o(x = -\infty) = E_o \sin\vartheta\,\hat{\underline{x}} + E_o \cos\vartheta\,\hat{\underline{y}} \tag{14}$$

so that $\vartheta = \tan^{-1}(E_{ox}/E_{oy})$ at $x = -\infty$. The influence of the x component of the electric field is then studied by varying ϑ, the angle between $\underset{\sim}{E}$ and $\hat{\underline{y}}$ at $x = -\infty$. The form of $E_{ox}(x)$ considered in the analysis is:

$$E_{ox}(x) = E_o \sin\vartheta\left(N_o/n_o(x)\right) \neq \text{constant} \tag{15}$$

We comment that Eq. (15) is an equilibrium solution which satisfies $\nabla\cdot\underline{J} = 0$ i.e., Eq. (4) or (6).

We consider two models with different initial electric field configurations to illustrate the effect of an inhomogeneous electric field. Model 1 has $E_{oy} = 10$ mV/m, $E_{ox} = 0$ (no velocity shear) while Model 2 takes $E_{ox}(-\infty) = 8.6$ mV/m and $E_{oy} = 5$ mV/m giving $\vartheta \simeq 60^o$. These electric field magnitudes are chosen to be typical of the high latitude diffuse auroral F-region ionosphere [Vickrey et al., 1980]. Figure 2a-2d shows the evolutions of the $\underline{E}$ x $\underline{B}$ instability using Model 1 (no velocity shear). Figure 2a shows the initial configuration which includes the small random perturbation. Figure 2b illustrates the linear regime at $t = 250$ sec ($\gamma t \simeq 5$) and shows unstable growth on the trailing side of the plasma enhancement as predicted by the linear result given by Eq. (12). One can

note the depletion jetting to the front side of the enhancement in analogy to the initial evolution of the $\underline{E} \times \underline{B}$ gradient drift instability in artificial ionospheric plasma clouds [Zabusky et al., 1973; Scannapieco et al., 1976]. Figure 2c gives the structure of the plasma enhancement at t = 500 sec and shows steepened fingers which are beginning to elongate. Finally Figure 2d displays the plasma enhancement at t = 650 sec in the fully nonlinear regime. The trailing edges of the principal fingers (striations) have steepened, become quasi-one dimensional and bifurcated. The length scales on Figure 2a-d are distorted with the depletions longer and narrower than is depicted.

Figure 3a-d give sample one-dimensional spatial power spectra at t = 0, 250, 650 sec Model 1. These power spectra are defined as follows

$$P(k_x) = \int dk_y \, \bar{P}(k_x,k_y)$$

$$P(k_y) = \int dk_x \, \bar{P}(k_x,k_y)$$

where $\bar{P}(k_x,k_y) \equiv (L_xL_y)^{-1}[\delta n(k_x,k_y)/N_o]^2$ is the spectral density, $\delta n = N-N_o$ with N_o the peak plasma enhancement density, and L_xL_y is the area of the numerical simulation plane. Figure 3a illustrates the power spectrum ($P(k_y)$ of the random perturbation used to initialize the $\underline{E} \times \underline{B}$ instability. Figure 3b shows the power spectrum $P(k_y)$ in the linear stage of the instability and compares favorably with the growth rate vs. k_y from local theory [Huba et al., 1983]. Figure 3c-3d gives the power spectra in the x- and y-directions, respectively, in the nonlinear regime at t = 650

sec. For both cases these power spectra are well-fitted with an inverse power law with spectral index $n_x \simeq 2$ for $2\pi/k_x$ between approximately 30 and 1 km and $n_y \simeq 2\text{-}2.5$ for $2\pi/k_y$ between 20 and 1 km.

Figures 4a-4d illustrate the evolution of the $\underline{E} \times \underline{B}$ instability with an inhomogeneous electric field using Model 2. Figure 4a gives the initial configuration which is identical to Fig. 2a. Figure 4b shows the isodensity contours of the plasma enhancement in the linear regime at t = 700 sec ($\gamma t \simeq 5$). Figure 4c gives the evolution at t = 900 sec and shows a distinct bending of the striations. Figure 4d details the $\underline{E} \times \underline{B}$ instability in the nonlinear regime at t = 1250 sec where one notes that the fingers (striations) are no longer primarily aligned with the flow. Similar morphologies are also observed for other velocity shears ($\vartheta = 30^{\circ}$).

Figures 5a-5c give sample power spectra for Model 2 in the linear and nonlinear regime at t = 425 and 1250 sec, respectively. Figure 5a illustrates the linear regime, shows the suppression of the shorter wavelength fluctuations in agreement with linear theory, eq. (10), [Perkins and Doles, 1975; Huba et al., 1983], and indicates a preferred scale size. Figure 5b gives a sample power spectrum in the y-direction, $P(k_y)$, and can be described by a power law $P(k_y) \sim k_y^{-n_y}$, $n_y \simeq 2\text{-}2.5$ in approximate agreement with the no shear case Model 1. The power spectrum in the x-direction $P(k_x)$ in the nonlinear regime is given in Fig. 5c and can also be described by a power law $P(k_x) \sim k_x^{-n_x}$, $n_x \simeq 2$. Similar power laws and spectral indices are also observed for the case where $\vartheta = 30^{\circ}$.

Figure 6 shows the evolution of the mean density profile along the x-axis (averaged over the y-direction) at t = 0, 700, 950 sec during the linear unstable stage of Model 2. Similar result are found for the case

$\vartheta = 30^{o}$. We show in the next section that this relaxation is responsible, in part, for the stabilization of the fastest growing linear modes.

4. QUASILINEAR THEORY

We present arguments for a quasilinear stabilization mechanism for the $\underline{E} \times \underline{B}$ instability with an inhomogeneous electric field. We show that the mean density gradient driving the instability is modified by an unstable spectrum of waves of finite amplitude. By dividing $N = n_o + \delta n$, $\underline{V}_e = \underline{V}_{eo} + \delta\underline{V}_e$, $\langle \delta n \rangle = \langle \delta V_e \rangle = 0$, into mean and oscillating parts (with $\langle\ \rangle$ denoting space and time average), the electron continuity equation (1) can be written

$$\frac{\partial n_o}{\partial t} = \frac{\partial \langle N \rangle}{\partial t} = - \nabla \cdot \langle \delta n\ \delta \underline{V}_e \rangle \tag{16}$$

$$\frac{\partial \delta n}{\partial t} + n_o \nabla \cdot \delta \underline{V}_e + \delta n \nabla \cdot \underline{V}_{eo} + \underline{V}_{eo} \cdot \nabla \delta n + \delta \underline{V}_e \cdot \nabla n_o$$

$$= \nabla \cdot \langle \delta n\ \delta \underline{V}_e \rangle - \nabla \cdot \delta n\ \delta \underline{V}_e \tag{17}$$

with $\langle \delta n\ \delta \underline{V}_e \rangle = (L_y)^{-1} \int d\underline{y}\ \delta n\ \delta \underline{V}_e = (L_y)^{-1} \int \frac{d\underline{k}_y}{(2\pi)^{-3}}\ \delta V_{e,-\underline{k}_y}\ \delta n_{\underline{k}_y}$ and $\delta \underline{V}_e \simeq - \frac{c}{B} \nabla \delta\phi \times \hat{z}$ and L_y is the length of the system in the y-direction. To find $\partial n_o / \partial t$ in Eq. (16) to lowest (quadratic) order in $\delta\phi$ one needs to compute δn to linear order in $\delta\phi$ using Eq. (17) which gives:

$$\delta n_{\underline{k}_y}(x) = - \frac{c}{B} k_y \frac{\partial n_o}{\partial x} \left[\omega - k_y V_{ey}(x)\right]^{-1} \delta\phi_{\underline{k}_y}(x) \tag{18}$$

giving

$$\langle \delta n \, \delta \underline{V}_e \rangle = (L_y)^{-1} \frac{ic}{B} \underline{k}_y \times \hat{z} \int \frac{dk_y}{(2\pi)^3} \delta\phi_{-\underline{k}_y} \delta n_{\underline{k}_y}$$

with $\delta n_{\underline{k}_y}$ given by (18). Inserting into (16) we find

$$\frac{\partial n_o}{\partial t} = - \frac{\partial}{\partial x} D(x) \frac{\partial}{\partial x} n_o \tag{19}$$

with $D(x) = \mathrm{Re} \left[i \frac{c^2}{B^2} \int dk_y \frac{k_y^2 I_{\underline{k}_y}(t)}{\omega - k_y V_{eo}(x)} \right]$

$$\simeq \frac{c^2}{B^2} \int dk_y \frac{I_{\underline{k}_y}(t)}{[\omega_r - kV_{eo}(x)]^2 + \gamma_k^2} \tag{20}$$

where $\omega = \omega_r + i\gamma$ has been used. The spectral energy density $I_{\underline{k}_y}(t) \equiv L_y^{-1} |\delta\phi_{\underline{k}_y}(t)|^2$ changes with time according to

$$\frac{\partial I_{\underline{k}_y}(t)}{\partial t} = 2\gamma_{\underline{k}}(t) I_{\underline{k}_y}(t) \tag{21}$$

Equation (19)-(21) provide a description of the quasilinear evolution of the $\underline{E} \times \underline{B}$ instability with an inhomogeneous electric field.

Assuming weakly growing modes, i.e., $\gamma_k^2 << |\omega_r - kV_{eo}(x)|^2$ the diffusion can be approximated by

$$D(x) \simeq \frac{c^2}{B^2} \int dk_y \, \gamma_{\underline{k}_y}^{-1} k_y^2 I_{\underline{k}_y}(t). \tag{22}$$

From the work of Huba et al. [1983] and the previous numerical simulation

results we observe that, although $\gamma_{\underline{k}_y}$ maximizes for preferred scale size given by $k_y L \sim O(1)$, the distribution of γ vs. k_y is broad. As a result, we take $\gamma_{\underline{k}_y}$ to be of the form

$$\gamma_{\underline{k}_y}(t) = \gamma_o(t)\exp\left[-(k_y - k_o)^2/k_w^2\right]$$

In addition, we assume

$$I_{\underline{k}_y}(t) = I_o(t)\exp\left[-(k_y - k_o)^2/k_w^2\right]$$

where $\gamma_o \simeq \zeta V_o/L$, $k_o \simeq \eta L^{-1}$, and k_w is the mean width of the distribution with $k_w \gtrsim k_o$. Here, ζ,η are constants of order unity [Huba et al., 1983. Inserting these expressions for $\gamma_{\underline{k}_y}$ and $I_{\underline{k}_y}$ into eq. (22) we take

$$D(x) \simeq \frac{c^2}{B^2}\gamma_o^{-1} I_o \int_{k_o - \frac{k_w}{2}}^{k_o + \frac{k_w}{2}} dk_y k_y^2$$

$$\simeq \frac{c^2}{B^2}\frac{L}{\zeta V_o} I_o \frac{k_w^3}{12} \tag{23}$$

For approximate nonlinear saturation of the fastest growing mode with wavenumber k_{max} we have

$$\gamma = \gamma_L - Dk_{max}^2 = 0 \tag{24}$$

Using eq. (23) in (24) we find

$$\left(\frac{\delta\phi}{\phi_o}\right)_{k=k_{max}} \simeq \frac{\sqrt{12}\,\zeta}{(k_{max}L)}\frac{1}{(k_w L)} \tag{25}$$

where $\phi_o = (BV_oL/c)$. From Huba et al. [1983], $\zeta \simeq 0.2$, $k_{max}L \simeq 1$, $k_wL \simeq 5$, which gives $\delta\phi/\phi_o \sim 0.11$ which is not inconsistent with the previous numerical simulation results in Sec. 3. After the initial mean density gradient has relaxed to a certain degree, small scale modes ($kL >> 1$) can become unstable leading to two-dimensional wave coupling processes which will determine the wave spectrum.

5. DISCUSSION AND SUMMARY

We have studied, using analytical and numerical techniques, the nonlinear evolution of the $\underline{E} \times \underline{B}$ instability with an inhomogeneous electric field. The principal results of this study are as follows:

1. The basic morphology and power spectra of the $\underline{E} \times \underline{B}$ instability with an inhomogeneous electric field in the nonlinear regime is similar to homogeneous (no shear) case.
2. Nonlinear effects destabilize the linearly stable modes associated with the $\underline{E} \times \underline{B}$ instability with inhomogeneous electric field.
3. Quasilinear mechanisms, in which the initial density gradient driving the inhomogeneous $\underline{E} \times \underline{B}$ instability is modified by a finite amplitude wave spectrum, can contribute to nonlinear stabilization.

Recently, large scale equatorward convecting plasma enhancements in the diffuse auroral F-region ionosphere have been identified and studied [Vickrey et al., 1980] using both radar and satellite measurements. Observed in regions of diffuse auroral particle precipitation and associated field aligned currents, these enhancements have overall latitudinal dimensions of a few hundred kilometers, contain relatively

steep poleward and equatorward edges, and have been shown to be approximately field-aligned resembling vertical slabs of ionization. Their occurrence, which is maximized in the evening-midnight sector, is apparently not strongly related to magnetic activity nor to E-region processes. The presence of plasma density irregularities associated with these enhancements has been verified using satellite scintillation studies [Fremouw et al., 1977; Rino et al., 1978; Vickrey et al., 1980]. The scintillation data have indicated that the electron density irregularities are structured like L-shell aligned sheets for irregularity scale sizes of approximately 1 km [Fremouw et al., 1977; Rino et al., 1980]. Moreover, the source region of these scintillation causing irregularities has been demonstrated to be latitude limited [Rino and Owen, 1980] and contained in a vertical slab of F region plasma. Keskinen and Ossakow [1982, 1983] showed that these convecting plasma enhancements can be destabilized by the $\underline{E} \times \underline{B}$ instability. Their results, using a homogeneous electric field, were not inconsistent with available experimental observations [Rino et al., 1978; Vickrey et al., 1980; Tsunoda and Vickrey, 1982]. The results of the present study, with an inhomogeneous electric field, may help explain the geometric (L-shell alignment) nature of these structures if one assumes the east-west (north-south) direction corresponds to the y(x)-axis. In this case, the fingerlike structures in the nonlinear regime of Model 2 would be approximately east-west or L-shell aligned.

These results are also applicable to the development of the $\underline{E} \times \underline{B}$ instability in artificially injected ionospheric plasma (barium) cloud releases. By including a self-consistent inhomogeneous electric field, we note that the time scales for striation formation and jetting is increased

compared to the homogeneous case. This effect will lead to an increase in striation onset time [McDonald et al., 1981]. However, in the nonlinear regime, our studies with an inhomogeneous electric field show similar morphologies and power spectra with respect to the homogeneous case.

Acknowledgments

This work was supported by the Defense Nuclear Agency and the Office of Naval Research.

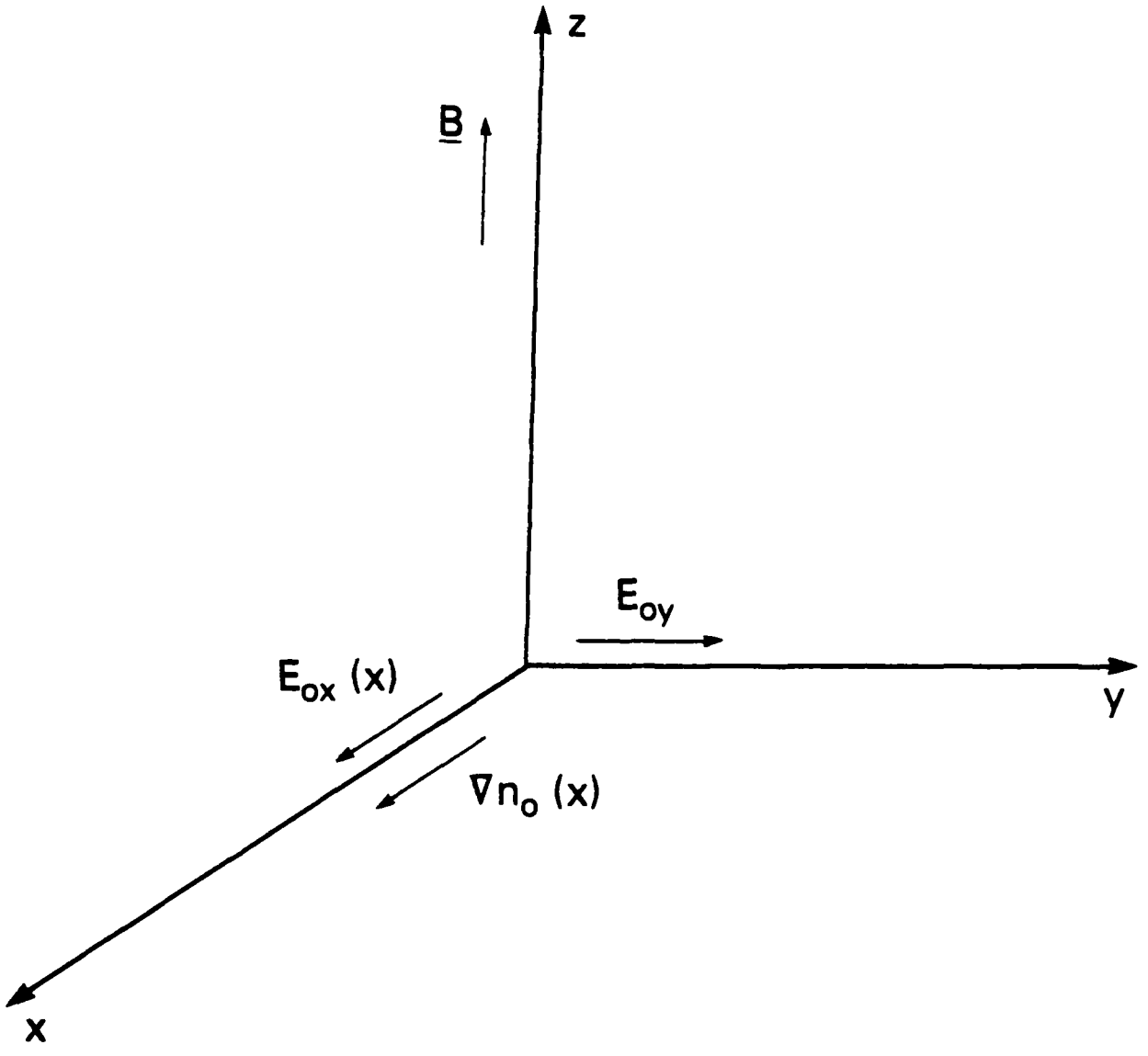

Fig. 1 — Basic geometry and coordinate system used in this analysis.

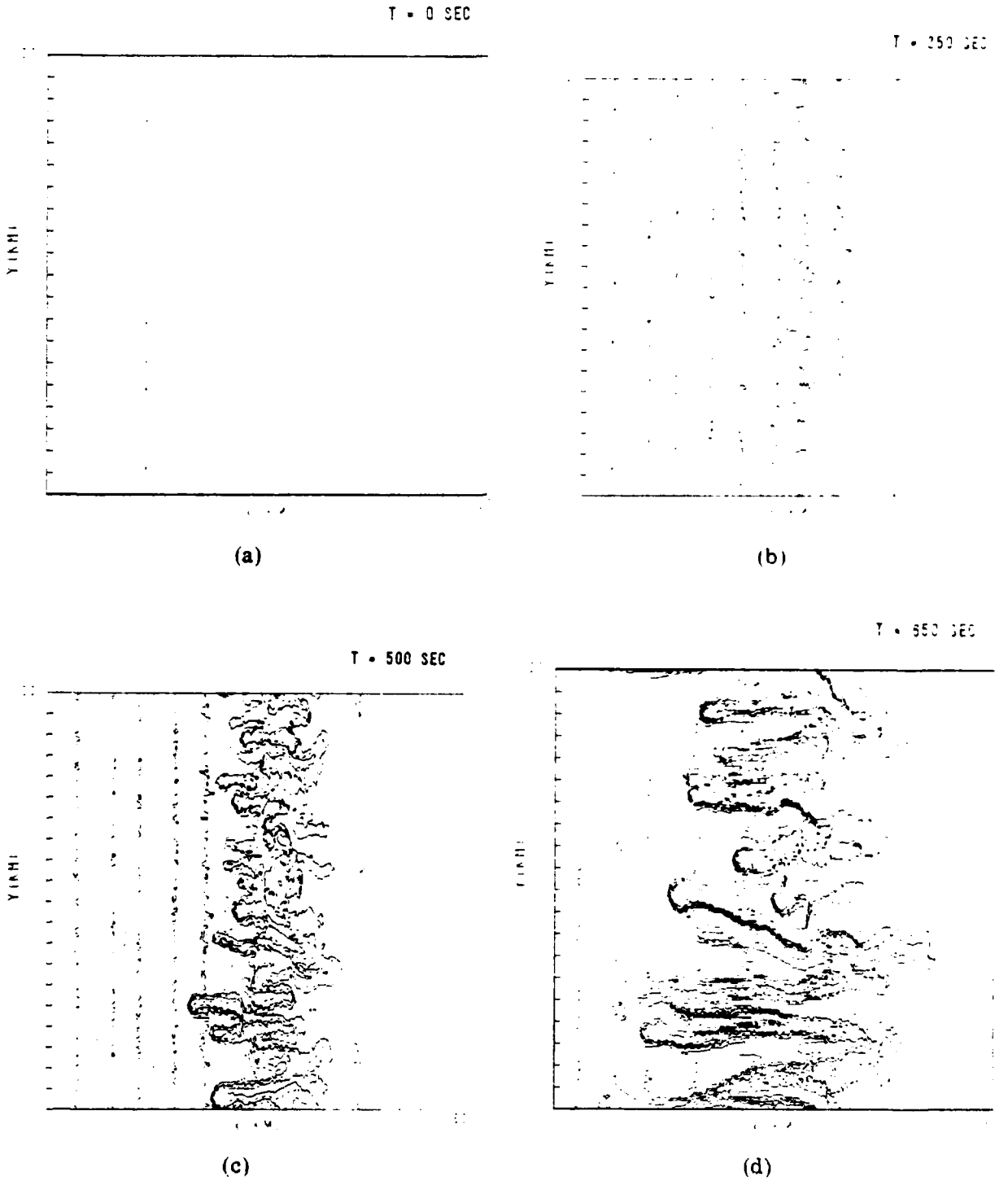

Fig. 2 — Real space isodensity contour plots of $n(x,y)/N_0$ for model 1 at (a) t = 0 sec, (b) t = 250 sec, (c) t = 500 sec, (d) t = 650 sec. The x-axis is compressed by a factor of 2.58. The distance between tic marks in the x-direction (y-direction) is 5 km (12.8 km). Eight contours are plotted in equal increments of 1.25 beginning at 1.25. The observer is looking downward along the magnetic field lines.

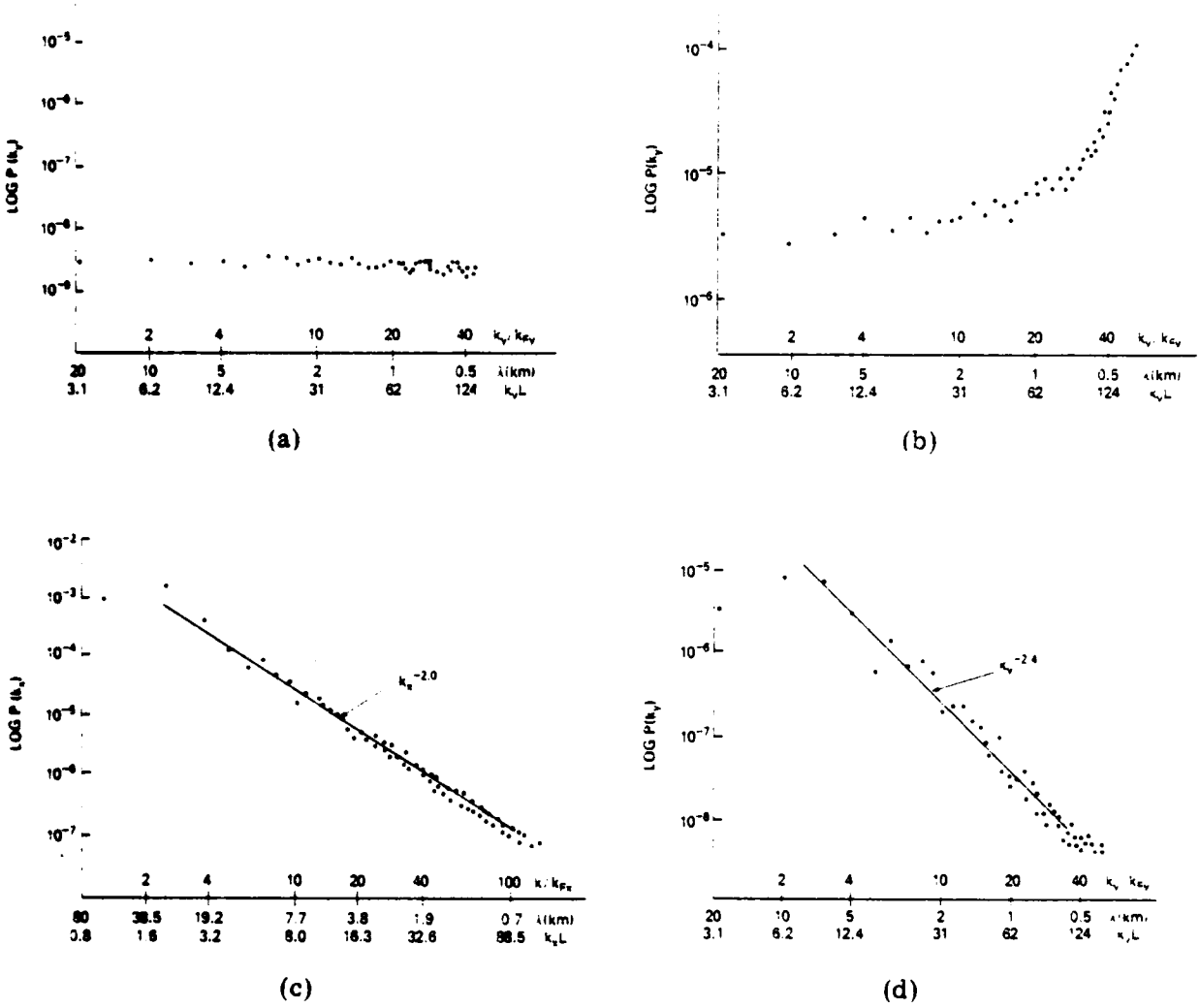

Fig. 3 — Sample one-dimensional power spectra for model 1 at (a) t = 0 sec, $P(k_y)$ (b) t = 250 sec, $P(k_y)$ (c) t = 650 sec, $P(k_x)$ (d) t = 650 sec, $P(k_y)$. Here $k_{Fx} = 2\pi/80$ km^{-1} and $k_{Fy} = 2\pi/20$ km^{-1}, the solid curve is a least squares fit to modes 2-80 in the x-direction and to modes 2-30 in the y-direction. The units of $P(k_x)$, $P(k_y)$ are km.

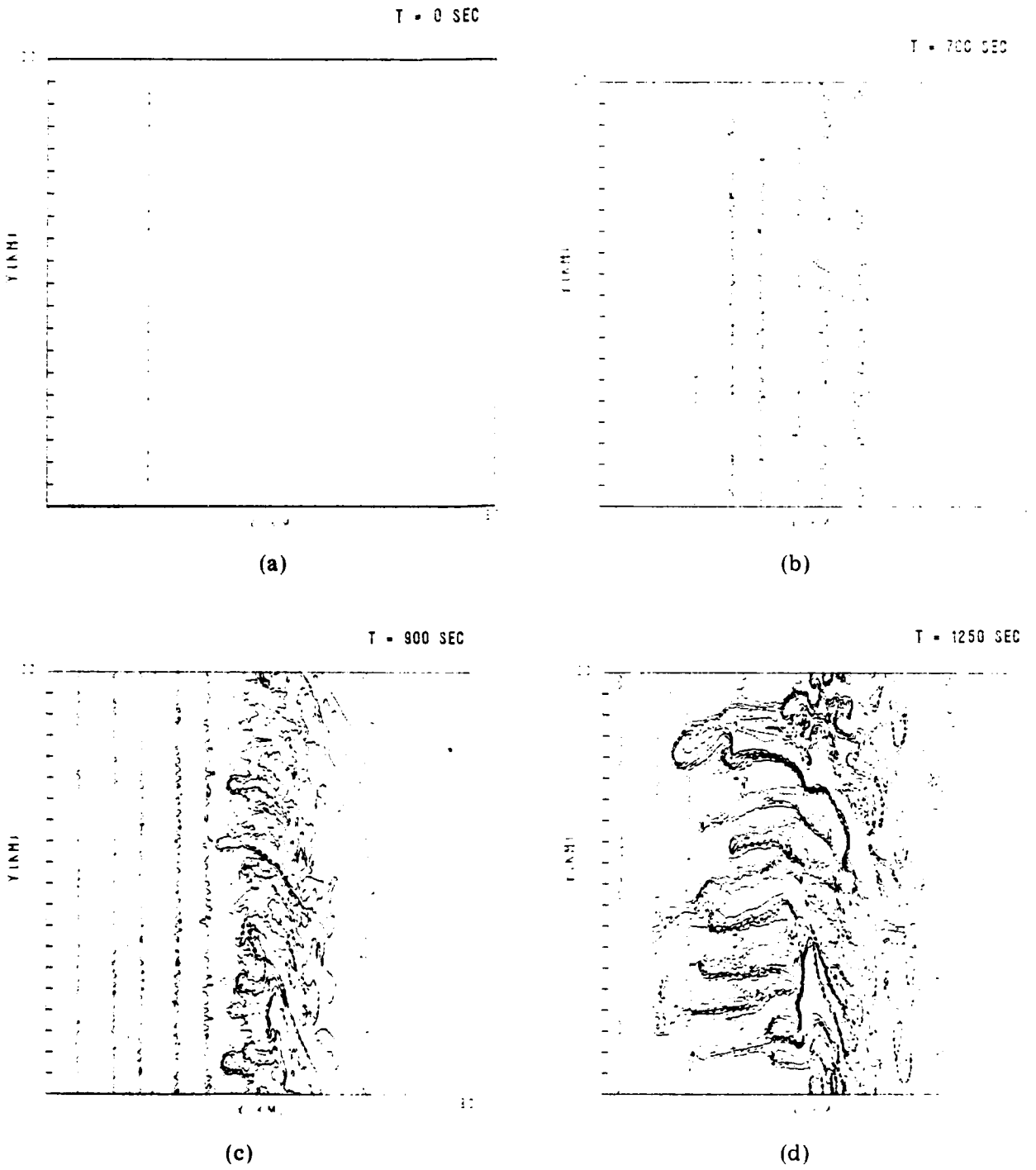

Fig. 4 — Real space isodensity contour plot of $n(x,y)/N_0$ for model 2 at (a) t = 0 sec, (b) t = 700 sec, (c) t = 900 sec, (d) t = 1250 sec, using the same format as Figure 2.

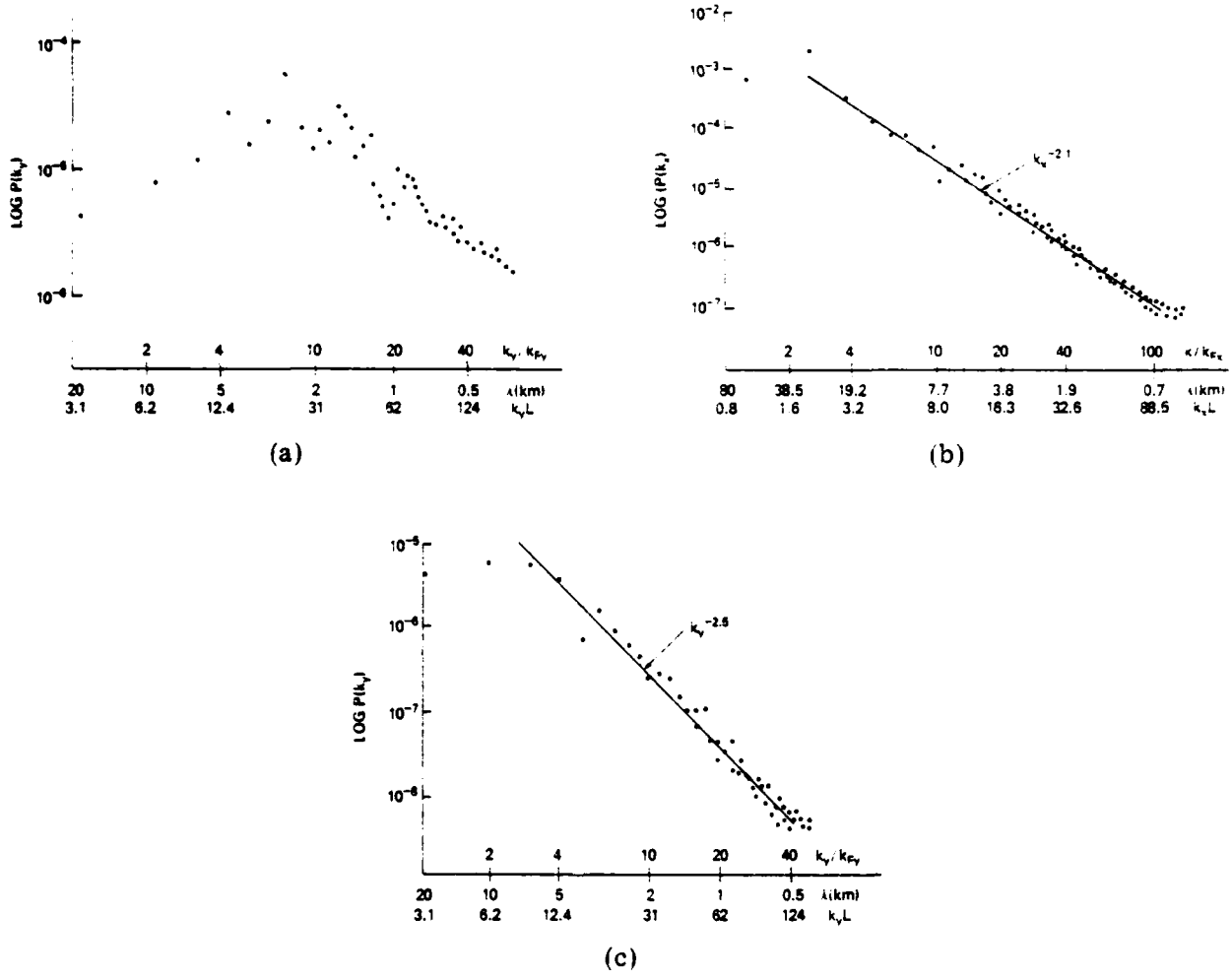

Fig. 5 — Sample one-dimensional power spectra for model 2 at (a) t = 425 sec, (b) t = 1250 sec, (c) t = 1250 sec in same format as Figure 3.

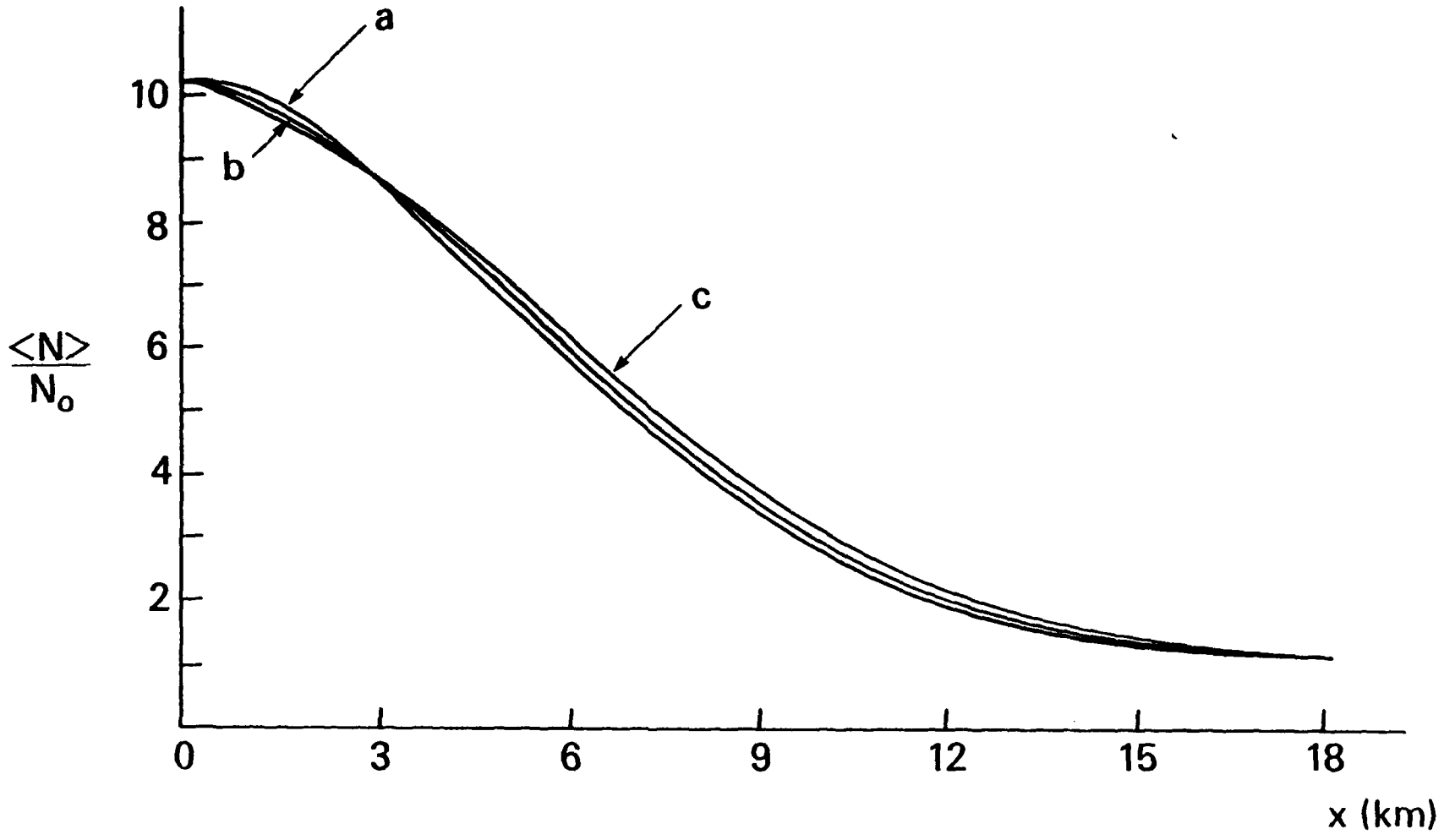

Fig. 6 — Mean density profiles along x-axis (averaged over y-axis) at several different times in the linear unstable stage of Model 2. Curve a,b,c correspond to t = 700, 950 sec. Distance x is measured from the maximum plasma enhancement density.

References

Chaturvedi, P.K. and S.L. Ossakow, Nonlinear Stabilization of the E x B Gradient Drift Instability in Ionospheric Plasma Clouds, J. Geophys. Res., 84, 419, 1979.

Fairfield, D.H., Electric and magnetic fields in the high-latitude magnetosphere, Rev. Geophys. Space Phys., 15, 285, 1977.

Haerendel, G., R. Lüst, and E. Rieger, Motion of artificial ion clouds in the upper atmosphere, Planet. Space Sci., 15, 1, 1967.

Hoh, F.C., Instability of Penning-Type Discharges, Phys. Fluids, 6, 1184, 1963.

Huba, J.D., S.L. Ossakow, P. Satyanarayana, and P.N. Guzdar, Linear theory of the E x B instability with an inhomogeneous electric field, J. Geophys. Res., 88, 425, 1983.

Keskinen, M.J., S.L. Ossakow, and P.K. Chaturvedi, Preliminary report of numerical simulations of intermediate wavelength E x B gradient drift instability in ionospheric plasma clouds, J. Geophys. Res., 85, 3485, 1980.

Keskinen, M.J. and S.L. Ossakow, Nonlinear evolution of plasma enhancements in the auroral ionosphere I: long wavelength irregularities, J. Geophys. Res., 87, 144, 1982.

Keskinen, M.J. and S.L. Ossakow, Nonlinear evolution of convecting plasma enhancements in the auroral ionosphere II: small scale irregularities, J. Geophys. Res., 88, 474, 1983.

Linson, L.M. and J.B. Workman, Formation of Striations in Ionospheric Plasma Clouds, J. Geophys. Res., 75, 3211, 1970.

McDonald, B.E., The Chebychev method for solving nonself-adjoint elliptic equations on a vector computer, J. Comput. Phys., 35, 147, 1980.

McDonald, B.E., S.L. Ossakow, S.T. Zalesak, and N.J. Zabusky, Scale Sizes and Lifetimes of F Region Plasma Cloud Striations as Determined by the Condition of Marginal Stability, J. Geophys. Res., 86, 5775, 1981.

Ossakow, S.L., P.K. Chaturvedi, and J.B. Workman, High-Altitude Limit of the Gradient Drift Instability, J. Geophys. Res., 83, 2691, 1978.

Perkins, F.W., N.J. Zabusky, and J.H. Doles III, Deformation and Striation of Plasma Clouds in the Ionosphere, 1, J. Geophys. Res., 78, 697, 1973.

Perkins, F.W. and J.H. Doles III, Velocity Shear and the E x B Instability, J. Geophys. Res., 80, 211, 1975.

Scannapieco, A.J., S.L. Ossakow, S.R. Goldman, and J.M. Pierre, Plasma Cloud Late Time Striation Spectra, J. Geophys. Res., 81, 6037, 1976.

Simon, A., Instability of a Partially Ionized Plasma in Crossed Electric and Magnetic Fields, Phys. Fluids, 6, 382, 1963.

Simon, A., Growth and Stability of Artificial Ion Clouds in the Ionosphere, J. Geophys. Res., 75, 6287, 1970.

Vickrey, J.F., C.L. Rino, and T.A. Potemra, Chatanika/Triad Observations of Unstable Ionization Enhancements in the Auroral F-Region, Geophys. Res. Lett., 7, 789, 1980.

Völk, H.J. and G. Haerendel, Striations in Ionospheric Ion Clouds, 1, J. Geophys. Res., 76, 4541, 1971.

Zabusky, N.J., J.H. Doles III and F.W. Perkins, Deformation and Striation of Plasma Clouds in the Ionosphere, 2. Numerical Simulation of a Nonlinear Two-Dimensional Model, J. Geophys. Res., 78, 711, 1973.

Zalesak, S.T., Fully multidimensional flux-corrected transport algorithms for fluids, J. Comput. Phys., 31, 335, 1979.

DISTRIBUTION LIST

DEPARTMENT OF DEFENSE

ASSISTANT SECRETARY OF DEFENSE
COMM, CMD, CONT 7 INTELL
WASHINGTON, D.C. 20301

DIRECTOR
COMMAND CONTROL TECHNICAL CENTER
PENTAGON RM BE 685
WASHINGTON, D.C. 20301
01CY ATTN C-650
01CY ATTN C-312 R. MASON

DIRECTOR
DEFENSE ADVANCED RSCH PROJ AGENCY
ARCHITECT BUILDING
1400 WILSON BLVD.
ARLINGTON, VA. 22209
01CY ATTN NUCLEAR MONITORING RESEARCH
01CY ATTN STRATEGIC TECH OFFICE

DEFENSE COMMUNICATION ENGINEER CENTER
1860 WIEHLE AVENUE
RESTON, VA. 22090
01CY ATTN CODE R410
01CY ATTN CODE R812

DEFENSE TECHNICAL INFORMATION CENTER
CAMERON STATION
ALEXANDRIA, VA. 22314
02CY

DIRECTOR
DEFENSE NUCLEAR AGENCY
WASHINGTON, D.C. 20305
01CY ATTN STVL
04CY ATTN TITL
01CY ATTN DDST
03CY ATTN RAAE

COMMANDER
FIELD COMMAND
DEFENSE NUCLEAR AGENCY
KIRTLAND, AFB, NM 87115
01CY ATTN FCPR

DIRECTOR
INTERSERVICE NUCLEAR WEAPONS SCHOOL
KIRTLAND AFB, NM 87115
01CY ATTN DOCUMENT CONTROL

JOINT CHIEFS OF STAFF
WASHINGTON, D.C. 20301
01CY ATTN J-3 WWMCCS EVALUATION OFFICE

DIRECTOR
JOINT STRAT TGT PLANNING STAFF
OFFUTT AFB
OMAHA, NB 68113
01CY ATTN JLTW-2
01CY ATTN JPST G. GOETZ

CHIEF
LIVERMORE DIVISION FLD COMMAND DNA
DEPARTMENT OF DEFENSE
LAWRENCE LIVERMORE LABORATORY
P.O. BOX 808
LIVERMORE, CA 94550
01CY ATTN FCPRL

COMMANDANT
NATO SCHOOL (SHAPE)
APO NEW YORK 09172
01CY ATTN U.S. DOCUMENTS OFFICER

UNDER SECY OF DEF FOR RSCH & ENGRG
DEPARTMENT OF DEFENSE
WASHINGTON, D.C. 20301
01CY ATTN STRATEGIC & SPACE SYSTEMS (OS)

WWMCCS SYSTEM ENGINEERING ORG
WASHINGTON, D.C. 20305
01CY ATTN R. CRAWFORD

COMMANDER/DIRECTOR
ATMOSPHERIC SCIENCES LABORATORY
U.S. ARMY ELECTRONICS COMMAND
WHITE SANDS MISSILE RANGE, NM 88002
01CY ATTN DELAS-EO F. NILES

DIRECTOR
BMD ADVANCED TECH CTR
HUNTSVILLE OFFICE
P.O. BOX 1500
HUNTSVILLE, AL 35807
01CY ATTN ATC-T MELVIN T. CAPPS
01CY ATTN ATC-O W. DAVIES
01CY ATTN ATC-R DON RUSS

PROGRAM MANAGER
BMD PROGRAM OFFICE
5001 EISENHOWER AVENUE
ALEXANDRIA, VA 22333
01CY ATTN DACS-BMT J. SHEA

CHIEF C-E- SERVICES DIVISION
U.S. ARMY COMMUNICATIONS CMD
PENTAGON RM 1B269
WASHINGTON, D.C. 20310
01CY ATTN C- E-SERVICES DIVISION

COMMANDER
FRADCOM TECHNICAL SUPPORT ACTIVITY
DEPARTMENT OF THE ARMY
FORT MONMOUTH, N.J. 07703
01CY ATTN DRSEL-NL-RD H. BENNET
01CY ATTN DRSEL-PL-ENV H. BOMKE
01CY ATTN J.E. QUIGLEY

COMMANDER
U.S. ARMY COMM-ELEC ENGRG INSTAL AGY
FT. HUACHUCA, AZ 85613
01CY ATTN CCC-EMEO GEORGE LANE

COMMANDER
U.S. ARMY FOREIGN SCIENCE & TECH CTR
220 7TH STREET, NE
CHARLOTTESVILLE, VA 22901
01CY ATTN DRXST-SD

COMMANDER
U.S. ARMY MATERIAL DEV & READINESS CMD
5001 EISENHOWER AVENUE
ALEXANDRIA, VA 22333
01CY ATTN DRCLDC J.A. BENDER

COMMANDER
U.S. ARMY NUCLEAR AND CHEMICAL AGENCY
7500 BACKLICK ROAD
BLDG 2073
SPRINGFIELD, VA 22150
01CY ATTN LIBRARY

DIRECTOR
U.S. ARMY BALLISTIC RESEARCH LABORATORY
ABERDEEN PROVING GROUND, MD 21005
01CY ATTN TECH LIBRARY EDWARD BAICY

COMMANDER
U.S. ARMY SATCOM AGENCY
FT. MONMOUTH, NJ 07703
01CY ATTN DOCUMENT CONTROL

COMMANDER
U.S. ARMY MISSILE INTELLIGENCE AGENCY
REDSTONE ARSENAL, AL 35809
01CY ATTN JIM GAMBLE

DIRECTOR
U.S. ARMY TRADOC SYSTEMS ANALYSIS ACTIVITY
WHITE SANDS MISSILE RANGE, NM 88002
01CY ATTN ATAA-SA
01CY ATTN TCC/F. PAYAN JR.
01CY ATTN ATTA-TAC LTC J. HESSE

COMMANDER
NAVAL ELECTRONIC SYSTEMS COMMAND
WASHINGTON, D.C. 20360
01CY ATTN NAVALEX 034 T. HUGHES
01CY ATTN PME 117
01CY ATTN PME 117-T
01CY ATTN CODE 5011

COMMANDING OFFICER
NAVAL INTELLIGENCE SUPPORT CTR
4301 SUITLAND ROAD, BLDG. 5
WASHINGTON, D.C. 20390
01CY ATTN MR. DUBBIN STIC 12
01CY ATTN NISC-50
01CY ATTN CODE 5404 J. GALET

COMMANDER
NAVAL OCCEAN SYSTEMS CENTER
SAN DIEGO, CA 92152
01CY ATTN J. FERGUSON

NAVAL RESEARCH LABORATORY
WASHINGTON, D.C. 20375
01CY ATTN CODE 4700 S. L. Ossakow
26 CYS IF UNCLASS. 1 CY IF CLASS)
01CY ATTN CODE 4701 I Vitkovitsky
01CY ATTN CODE 4780 J. Huba (100
CYS IF UNCLASS, 1 CY IF CLASS)
01CY ATTN CODE 7500
01CY ATTN CODE 7550
01CY ATTN CODE 7580
01CY ATTN CODE 7551
01CY ATTN CODE 7555
01CY ATTN CODE 4730 E. MCLEAN
01CY ATTN CODE 4108
01CY ATTN CODE 4730 B. RIPIN
20CY ATTN CODE 2628

COMMANDER
NAVAL SEA SYSTEMS COMMAND
WASHINGTON, D.C. 20362
01CY ATTN CAPT R. PITKIN

COMMANDER
NAVAL SPACE SURVEILLANCE SYSTEM
DAHLGREN, VA 22448
01CY ATTN CAPT J.H. BURTON

OFFICER-IN-CHARGE
NAVAL SURFACE WEAPONS CENTER
WHITE OAK, SILVER SPRING, MD 20910
01CY ATTN CODE F31

DIRECTOR
STRATEGIC SYSTEMS PROJECT OFFICE
DEPARTMENT OF THE NAVY
WASHINGTON, D.C. 20376
01CY ATTN NSP-2141
01CY ATTN NSSP-2722 FRED WIMBERLY

COMMANDER
NAVAL SURFACE WEAPONS CENTER
DAHLGREN LABORATORY
DAHLGREN, VA 22448
01CY ATTN CODE DF-14 R. BUTLER

OFFICER OF NAVAL RESEARCH
ARLINGTON, VA 22217
01CY ATTN CODE 465
01CY ATTN CODE 461
01CY ATTN CODE 402
01CY ATTN CODE 420
01CY ATTN CODE 421

COMMANDER
AEROSPACE DEFENSE COMMAND/DC
DEPARTMENT OF THE AIR FORCE
ENT AFB, CO 80912
01CY ATTN DC MR. LONG

COMMANDER
AEROSPACE DEFENSE COMMAND/XPD
DEPARTMENT OF THE AIR FORCE
ENT AFB, CO 80912
01CY ATTN XPDQQ
01CY ATTN XP

AIR FORCE GEOPHYSICS LABORATORY
HANSCOM AFB, MA 01731
01CY ATTN OPR HAROLD GARDNER
01CY ATTN LKB KENNETH S.W. CHAMPION
01CY ATTN OPR ALVA T. STAIR
01CY ATTN PHD JURGEN BUCHAU
01CY ATTN PHD JOHN P. MULLEN

AF WEAPONS LABORATORY
KIRTLAND AFT, NM 87117
01CY ATTN SUL
01CY ATTN CA ARTHUR H. GUENTHER
01CY ATTN NTYCE 1LT. G. KRAJEI

AFTAC
PATRICK AFB, FL 32925
01CY ATTN TF/MAJ WILEY
01CY ATTN TN

AIR FORCE AVIONICS LABORATORY
WRIGHT-PATTERSON AFB, OH 45433
01CY ATTN AAD WADE HUNT
01CY ATTN AAD ALLEN JOHNSON

DEPUTY CHIEF OF STAFF
RESEARCH, DEVELOPMENT, & ACQ
DEPARTMENT OF THE AIR FORCE
WASHINGTON, D.C. 20330
01CY ATTN AFRDQ

HEADQUARTERS
ELECTRONIC SYSTEMS DIVISION
DEPARTMENT OF THE AIR FORCE
HANSCOM AFB, MA 01731
01CY ATTN J. DEAS

HEADQUARTERS
ELECTRONIC SYSTEMS DIVISION/YSEA
DEPARTMENT OF THE AIR FORCE
HANSCOM AFB, MA 01732
01CY ATTN YSEA

HEADQUARTERS
ELECTRONIC SYSTEMS DIVISION/DC
DEPARTMENT OF THE AIR FORCE
HANSCOM AFB, MA 01731
01CY ATTN DCKC MAJ J.C. CLARK

COMMANDER
FOREIGN TECHNOLOGY DIVISION, AFSC
WRIGHT-PATTERSON AFB, OH 45433
01CY ATTN NICD LIBRARY
01CY ATTN ETDP B. BALLARD

COMMANDER
ROME AIR DEVELOPMENT CENTER, AFSC
GRIFFISS AFB, NY 13441
01CY ATTN DOC LIBRARY/TSLD
01CY ATTN OCSE V. COYNE

SAMSO/SZ
POST OFFICE BOX 92960
WORLDWAY POSTAL CENTER
LOS ANGELES, CA 90009
(SPACE DEFENSE SYSTEMS)
01CY ATTN SZJ

STRATEGIC AIR COMMAND/XPFS
OFFUTT AFB, NB 68113
01CY ATTN ADWATE MAJ BRUCE BAUER
01CY ATTN NRT
01CY ATTN DOK CHIEF SCIENTIST

SAMSO/SK
P.O. BOX 92960
WORLDWAY POSTAL CENTER
LOS ANGELES, CA 90009
01CY ATTN SKA (SPACE COMM SYSTEMS)
M. CLAVIN

SAMSO/MN
NORTON AFB, CA 92409
(MINUTEMAN)
01CY ATTN MNNL

COMMANDER
ROME AIR DEVELOPMENT CENTER, AFSC
HANSCOM AFB, MA 01731
01CY ATTN EEP A. LORENTZEN

DEPARTMENT OF ENERGY
LIBRARY ROOM G-042
WASHINGTON, D.C. 20545
01CY ATTN DOC CON FOR A. LABOWITZ

DEPARTMENT OF ENERGY
ALBUQUERQUE OPERATIONS OFFICE
P.O. BOX 5400
ALBUQUERQUE, NM 87115
01CY ATTN DOC CON FOR D. SHERWOOD

EG&G, INC.
LOS ALAMOS DIVISION
P.O. BOX 809
LOS ALAMOS, NM 85544
01CY ATTN DOC CON FOR J. BREEDLOVE

UNIVERSITY OF CALIFORNIA
LAWRENCE LIVERMORE LABORATORY
P.O. BOX 808
LIVERMORE, CA 94550
01CY ATTN DOC CON FOR TECH INFO DEPT
01CY ATTN DOC CON FOR L-389 R. OTT
01CY ATTN DOC CON FOR L-31 R. HAGER
01CY ATTN DOC CON FOR L-46 F. SEWARD

LOS ALAMOS NATIONAL LABORATORY
P.O. BOX 1663
LOS ALAMOS, NM 87545
01CY ATTN DOC CON FOR J. WOLCOTT
01CY ATTN DOC CON FOR R.F. TASCHEK
01CY ATTN DOC CON FOR E. JONES
01CY ATTN DOC CON FOR J. MALIK
01CY ATTN DOC CON FOR R. JEFFRIES
01CY ATTN DOC CON FOR J. ZINN
01CY ATTN DOC CON FOR P. KEATON
01CY ATTN DOC CON FOR D. WESTERVELT
01CY ATTN D. SAPPENFIELD

SANDIA LABORATORIES
P.O. BOX 5800
ALBUQUERQUE, NM 87115
01CY ATTN DOC CON FOR W. BROWN
01CY ATTN DOC CON FOR A. THORNBROUGH
01CY ATTN DOC CON FOR T. WRIGHT
01CY ATTN DOC CON FOR D. DAHLGREN
01CY ATTN DOC CON FOR 3141
01CY ATTN DOC CON FOR SPACE PROJECT DIV

SANDIA LABORATORIES
LIVERMORE LABORATORY
P.O. BOX 969
LIVERMORE, CA 94550
01CY ATTN DOC CON FOR B. MURPHEY
01CY ATTN DOC CON FOR T. COOK

OFFICE OF MILITARY APPLICATION
DEPARTMENT OF ENERGY
WASHINGTON, D.C. 20545
01CY ATTN DOC CON DR. YO SONG

OTHER GOVERNMENT

DEPARTMENT OF COMMERCE
NATIONAL BUREAU OF STANDARDS
WASHINGTON, D.C. 20234
01CY (ALL CORRES: ATTN SEC OFFICER FOR)

INSTITUTE FOR TELECOM SCIENCES
NATIONAL TELECOMMUNICATIONS & INFO ADMIN
BOULDER, CO 80303
01CY ATTN A. JEAN (UNCLASS ONLY)
01CY ATTN W. UTLAUT
01CY ATTN D. CROMBIE
01CY ATTN L. BERRY

NATIONAL OCEANIC & ATMOSPHERIC ADMIN
ENVIRONMENTAL RESEARCH LABORATORIES
DEPARTMENT OF COMMERCE
BOULDER, CO 80302
01CY ATTN R. GRUBB
01CY ATTN AERONOMY LAB G. REID

DEPARTMENT OF DEFENSE CONTRACTORS

AEROSPACE CORPORATION
P.O. BOX 92957
LOS ANGELES, CA 90009
01CY ATTN I. GARFUNKEL
01CY ATTN T. SALMI
01CY ATTN V. JOSEPHSON
01CY ATTN S. BOWER
01CY ATTN D. OLSEN

ANALYTICAL SYSTEMS ENGINEERING CORP
5 OLD CONCORD ROAD
BURLINGTON, MA 01803
01CY ATTN RADIO SCIENCES

AUSTIN RESEARCH ASSOC., INC.
1901 RUTLAND DRIVE
AUSTIN, TX 78758
01CY ATTN L. SLOAN
01CY ATTN R. THOMPSON

BERKELEY RESEARCH ASSOCIATES, INC.
P.O. BOX 983
BERKELEY, CA 94701
01CY ATTN J. WORKMAN
01CY ATTN C. PRETTIE
01CY ATTN S. BRECHT

BOEING COMPANY, THE
P.O. BOX 3707
SEATTLE, WA 98124
01CY ATTN G. KEISTER
01CY ATTN D. MURRAY
01CY ATTN G. HALL
01CY ATTN J. KENNEY

CHARLES STARK DRAPER LABORATORY, INC.
555 TECHNOLOGY SQUARE
CAMBRIDGE, MA 02139
01CY ATTN D.B. COX
01CY ATTN J.P. GILMORE

COMSAT LABORATORIES
LINTHICUM ROAD
CLARKSBURG, MD 20734
01CY ATTN G. HYDE

CORNELL UNIVERSITY
DEPARTMENT OF ELECTRICAL ENGINEERING
ITHACA, NY 14850
01CY ATTN D.T. FARLEY, JR.

ELECTROSPACE SYSTEMS, INC.
BOX 1359
RICHARDSON, TX 75080
01CY ATTN H. LOGSTON
01CY ATTN SECURITY (PAUL PHILLIPS)

EOS TECHNOLOGIES, INC.
606 Wilshire Blvd.
Santa Monica, Calif 90401
01CY ATTN C.B. GABBARD

ESL, INC.
495 JAVA DRIVE
SUNNYVALE, CA 94086
01CY ATTN J. ROBERTS
01CY ATTN JAMES MARSHALL

GENERAL ELECTRIC COMPANY
SPACE DIVISION
VALLEY FORGE SPACE CENTER
GODDARD BLVD KING OF PRUSSIA
P.O. BOX 8555
PHILADELPHIA, PA 19101
01CY ATTN M.H. BORTNER SPACE SCI LAB

GENERAL ELECTRIC COMPANY
P.O. BOX 1122
SYRACUSE, NY 13201
01CY ATTN F. REIBERT

GENERAL ELECTRIC TECH SERVICES CO., INC.
HMES
COURT STREET
SYRACUSE, NY 13201
01CY ATTN G. MILLMAN

GEOPHYSICAL INSTITUTE
UNIVERSITY OF ALASKA
FAIRBANKS, AK 99701
(ALL CLASS ATTN: SECURITY OFFICER)
01CY ATTN T.N. DAVIS (UNCLASS ONLY)
01CY ATTN TECHNICAL LIBRARY
01CY ATTN NEAL BROWN (UNCLASS ONLY)

GTE SYLVANIA, INC.
ELECTRONICS SYSTEMS GRP-EASTERN DIV
77 A STREET
NEEDHAM, MA 02194
01CY ATTN DICK STEINHOF

HSS, INC.
2 ALFRED CIRCLE
BEDFORD, MA 01730
01CY ATTN DONALD HANSEN

ILLINOIS, UNIVERSITY OF
107 COBLE HALL
150 DAVENPORT HOUSE
CHAMPAIGN, IL 61820
(ALL CORRES ATTN DAN MCCLELLAND)
01CY ATTN K. YEH

INSTITUTE FOR DEFENSE ANALYSES
1801 NO. BEAUREGARD STREET
ALEXANDRIA, VA 22311
01CY ATTN J.M. AEIN
01CY ATTN ERNEST BAUER
01CY ATTN HANS WOLFARD
01CY ATTN JOEL BENGSTON

INTL TEL & TELEGRAPH CORPORATION
500 WASHINGTON AVENUE
NUTLEY, NJ 07110
01CY ATTN TECHNICAL LIBRARY

JAYCOR
11011 TORREYANA ROAD
P.O. BOX 85154
SAN DIEGO, CA 92138
01CY ATTN J.L. SPERLING

JOHNS HOPKINS UNIVERSITY
APPLIED PHYSICS LABORATORY
JOHNS HOPKINS ROAD
LAUREL, MD 20810
01CY ATTN DOCUMENT LIBRARIAN
01CY ATTN THOMAS POTEMRA
01CY ATTN JOHN DASSOULAS

KAMAN SCIENCES CORP
P.O. BOX 7463
COLORADO SPRINGS, CO 80933
01CY ATTN T. MEAGHER

KAMAN TEMPO-CENTER FOR ADVANCED STUDIES
816 STATE STREET (P.O DRAWER QQ)
SANTA BARBARA, CA 93102
01CY ATTN DASIAC
01CY ATTN WARREN S. KNAPP
01CY ATTN WILLIAM MCNAMARA
01CY ATTN B. GAMBILL

LINKABIT CORP
10453 ROSELLE
SAN DIEGO, CA 92121
01CY ATTN IRWIN JACOBS

LOCKHEED MISSILES & SPACE CO., INC
P.O. BOX 504
SUNNYVALE, CA 94088
01CY ATTN DEPT 60-12
01CY ATTN D.R. CHURCHILL

LOCKHEED MISSILES & SPACE CO., INC.
3251 HANOVER STREET
PALO ALTO, CA 94304
01CY ATTN MARTIN WALT DEPT 52-12
01CY ATTN W.L. IMHOF DEPT 52-12
01CY ATTN RICHARD G. JOHNSON DEPT 52-12
01CY ATTN J.B. CLADIS DEPT 52-12

MARTIN MARIETTA CORP
ORLANDO DIVISION
P.O. BOX 5837
ORLANDO, FL 32805
01CY ATTN R. HEFFNER

M.I.T. LINCOLN LABORATORY
P.O. BOX 73
LEXINGTON, MA 02173
01CY ATTN DAVID M. TOWLE
01CY ATTN L. LOUGHLIN
01CY ATTN D. CLARK

MCDONNEL DOUGLAS CORPORATION
5301 BOLSA AVENUE
HUNTINGTON BEACH, CA 92647
01CY ATTN N. HARRIS
01CY ATTN J. MOULE
01CY ATTN GEORGE MROZ
01CY ATTN W. OLSON
01CY ATTN R.W. HALPRIN
01CY ATTN TECHNICAL LIBRARY SERVICES

MISSION RESEARCH CORPORATION
735 STATE STREET
SANTA BARBARA, CA 93101
01CY ATTN P. FISCHER
01CY ATTN W.F. CREVIER
01CY ATTN STEVEN L. GUTSCHE
01CY ATTN R. BOGUSCH
01CY ATTN R. HENDRICK
01CY ATTN RALPH KILB
01CY ATTN DAVE SOWLE
01CY ATTN F. FAJEN
01CY ATTN M. SCHEIBE
01CY ATTN CONRAD L. LONGMIRE
01CY ATTN B. WHITE

MISSION RESEARCH CORP.
1720 RANDOLPH ROAD, S.E.
ALBUQUERQUE, NEW MEXICO 87106
01CY R. STELLINGWERF
01CY M. ALME
01CY L. WRIGHT

MITRE CORPORATION, THE
P.O. BOX 208
BEDFORD, MA 01730
01CY ATTN JOHN MORGANSTERN
01CY ATTN G. HARDING
01CY ATTN C.E. CALLAHAN

MITRE CORP
WESTGATE RESEARCH PARK
1820 DOLLY MADISON BLVD
MCLEAN, VA 22101
01CY ATTN W. HALL
01CY ATTN W. FOSTER

PACIFIC-SIERRA RESEARCH CORP
12340 SANTA MONICA BLVD.
LOS ANGELES, CA 90025
01CY ATTN E.C. FIELD, JR.

PENNSYLVANIA STATE UNIVERSITY
IONOSPHERE RESEARCH LAB
318 ELECTRICAL ENGINEERING EAST
UNIVERSITY PARK, PA 16802
(NO CLASS TO THIS ADDRESS)
01CY ATTN IONOSPHERIC RESEARCH LAB

PHOTOMETRICS, INC.
4 ARROW DRIVE
WOBURN, MA 01801
01CY ATTN IRVING L. KOFSKY

PHYSICAL DYNAMICS, INC.
P.O. BOX 3027
BELLEVUE, WA 98009
01CY ATTN E.J. FREMOUW

PHYSICAL DYNAMICS, INC.
P.O. BOX 10367
OAKLAND, CA 94610
ATTN A. THOMSON

R & D ASSOCIATES
P.O. BOX 9695
MARINA DEL REY, CA 90291
01CY ATTN FORREST GILMORE
01CY ATTN WILLIAM B. WRIGHT, JR.
01CY ATTN ROBERT F. LELEVIER
01CY ATTN WILLIAM J. KARZAS
01CY ATTN H. ORY
01CY ATTN C. MACDONALD
01CY ATTN R. TURCO
01CY ATTN L. DeRAND
01CY ATTN W. TSAI

RAND CORPORATION, THE
1700 MAIN STREET
SANTA MONICA, CA 90406
01CY ATTN CULLEN CRAIN
01CY ATTN ED BEDROZIAN

RAYTHEON CO.
528 BOSTON POST ROAD
SUDBURY, MA 01776
01CY ATTN BARBARA ADAMS

RIVERSIDE RESEARCH INSTITUTE
330 WEST 42nd STREET
NEW YORK, NY 10036
01CY ATTN VINCE TRAPANI

SCIENCE APPLICATIONS, INC.
1150 PROSPECT PLAZA
LA JOLLA, CA 92037
01CY ATTN LEWIS M. LINSON
01CY ATTN DANIEL A. HAMLIN
01CY ATTN E. FRIEMAN
01CY ATTN E.A. STRAKER
01CY ATTN CURTIS A. SMITH
01CY ATTN JACK MCDOUGALL

SCIENCE APPLICATIONS, INC
1710 GOODRIDGE DR.
MCLEAN, VA 22102
ATTN: J. COCKAYNE

SRI INTERNATIONAL
333 RAVENSWOOD AVENUE
MENLO PARK, CA 94025
01CY ATTN DONALD NEILSON
01CY ATTN ALAN BURNS
01CY ATTN G. SMITH
01CY ATTN R. TSUNODA
01CY ATTN DAVID A. JOHNSON
01CY ATTN WALTER G. CHESNUT
01CY ATTN CHARLES L. RINO
01CY ATTN WALTER JAYE
01CY ATTN J. VICKREY
01CY ATTN RAY L. LEADABRAND
01CY ATTN G. CARPENTER
01CY ATTN G. PRICE
01CY ATTN R. LIVINGSTON
01CY ATTN V. GONZALES
01CY ATTN D. MCDANIEL

TECHNOLOGY INTERNATIONAL CORP
75 WIGGINS AVENUE
BEDFORD, MA 01730
01CY ATTN W.P. BOQUIST

TOYON RESEARCH CO.
P.O. Box 6890
SANTA BARBARA, CA 93111
01CY ATTN JOHN ISE, JR.
01CY ATTN JOEL GARBARINO

TRW DEFENSE & SPACE SYS GROUP
ONE SPACE PARK
REDONDO BEACH, CA 90278
01CY ATTN R. K. PLEBUCH
01CY ATTN S. ALTSCHULER
01CY ATTN D. DEE
01CY ATTN D/ STOCKWELL
SNTF/1575

VISIDYNE
SOUTH BEDFORD STREET
BURLINGTON, MASS 01803
01CY ATTN W. REIDY
01CY ATTN J. CARPENTER
01CY ATTN C. HUMPHREY

IONOSPHERIC MODELING DISTRIBUTION LIST
(UNCLASSIFIED ONLY)

PLEASE DISTRIBUTE ONE COPY TO EACH OF THE FOLLOWING PEOPLE (UNLESS OTHERWISE NOTED)

NAVAL RESEARCH LABORATORY
WASHINGTON, D.C. 20375
Dr. P. MANGE - CODE 4101
Dr. P. GOODMAN - CODE 4180

A.F. GEOPHYSICS LABORATORY
L.G. HANSCOM FIELD
BEDFORD, MA 01730
DR. T. ELKINS
DR. W. SWIDER
MRS. R. SAGALYN
DR. J.M. FORBES
DR. T.J. KENESHEA
DR. W. BURKE
DR. H. CARLSON
DR. J. JASPERSE

BOSTON UNIVERSITY
DEPARTMENT OF ASTRONOMY
BOSTON, MA 02215
DR. J. AARONS

CORNELL UNIVERSITY
ITHACA, NY 14850
DR. W.E. SWARTZ
DR. D. FARLEY
DR. M. KELLEY

HARVARD UNIVERSITY
HARVARD SQUARE
CAMBRIDGE, MA 02138
DR. M.B. McELROY
DR. R. LINDZEN

INSTITUTE FOR DEFENSE ANALYSIS
400 ARMY/NAVY DRIVE
ARLINGTON, VA 22202
DR. E. BAUER

MASSACHUSETTS INSTITUTE OF TECHNOLOGY
PLASMA FUSION CENTER
LIBRARY, NW16-262
CAMBRIDGE, MA 02139

NASA
GODDARD SPACE FLIGHT CENTER
GREENBELT, MD 20771
DR. K. MAEDA
DR. S. CURTIS
DR. M. DUBIN
DR. N. MAYNARD - CODE 696

COMMANDER
NAVAL AIR SYSTEMS COMMAND
DEPARTMENT OF THE NAVY
WASHINGTON, D.C. 20360
DR. T. CZUBA

COMMANDER
NAVAL OCEAN SYSTEMS CENTER
SAN DIEGO, CA 92152
MR. R. ROSE - CODE 5321

NOAA
DIRECTOR OF SPACE AND ENVIRONMENTAL LABORATORY
BOULDER, CO 80302
DR. A. GLENN JEAN
DR. G.W. ADAMS
DR. D.N. ANDERSON
DR. K. DAVIES
DR. R.F. DONNELLY

OFFICE OF NAVAL RESEARCH
800 NORTH QUINCY STREET
ARLINGTON, VA 22217
DR. G. JOINER

PENNSYLVANIA STATE UNIVERSITY
UNIVERSITY PARK, PA 16802
DR. J.S. NISBET
DR. P.R. ROHRBAUGH
DR. L.A. CARPENTER
DR. M. LEE
DR. R. DIVANY
DR. P. BENNETT
DR. F. KLEVANS

SCIENCE APPLICATIONS, INC.
1150 PROSPECT PLAZA
LA JOLLA, CA 92037
DR. D.A. HAMLIN
DR. E. FRIEMAN

STANFORD UNIVERSITY
STANFORD, CA 94305
DR. P.M. BANKS

U.S. ARMY ABERDEEN RESEARCH
AND DEVELOPMENT CENTER
BALLISTIC RESEARCH LABORATORY
ABERDEEN, MD
DR. J. HEIMERL

GEOPHYSICAL INSTITUTE
UNIVERSITY OF ALASKA
FAIRBANKS, AK 99701
DR. L.E. LEE

UNIVERSITY OF CALIFORNIA,
BERKELEY
BERKELEY, CA 94720
DR. M. HUDSON

UNIVERSITY OF CALIFORNIA
LOS ALAMOS SCIENTIFIC LABORATORY
J-10, MS-664
LOS ALAMOS, NM 87545
DR. M. PONGRATZ
DR. D. SIMONS
DR. G. BARASCH
DR. L. DUNCAN
DR. P. BERNHARDT
DR. S.P. GARY

UNIVERSITY OF MARYLAND
COLLEGE PARK, MD 20740
DR. K. PAPADOPOULOS
DR. E. OTT

JOHNS HOPKINS UNIVERSITY
APPLIED PHYSICS LABORATORY
JOHNS HOPKINS ROAD
LAUREL, MD 20810
DR. R. GREENWALD
DR. C. MENG

UNIVERSITY OF PITTSBURGH
PITTSBURGH, PA 15213
DR. N. ZABUSKY
DR. M. BIONDI
DR. E. OVERMAN

UNIVERSITY OF TEXAS
AT DALLAS
CENTER FOR RESEARCH SCIENCES
P.O. BOX 688
RICHARDSON, TX 75080
DR. R. HEELIS
DR. W. HANSON
DR. J.P. McCLURE

UTAH STATE UNIVERSITY
4TH AND 8TH STREETS
LOGAN, UTAH 84322
DR. R. HARRIS
DR. K. BAKER
DR. R. SCHUNK
DR. J. ST.-MAURICE

PHYSICAL RESEARCH LABORATORY
PLASMA PHYSICS PROGRAMME
AHMEDABAD 380 009
INDIA
P.J. PATHAK, LIBRARIAN

LABORATORY FOR PLASMA AND
FUSION ENERGY STUDIES
UNIVERSITY OF MARYLAND
COLLEGE PARK, MD 20742
JHAN VARYAN HELLMAN,
REFERENCE LIBRARIAN

END

FILMED

02 — 84

DTIC